

Gas reservoir of a hyper-luminous QSO at $z = 2.6^{\star}$

C. Feruglio^{1,2}, A. Bongiorno², F. Fiore², M. Krips¹, M. Brusa^{3,4,5}, E. Daddi⁶, I. Gavignaud⁷, R. Maiolino⁸, E. Piconcelli², M. Sargent⁹, C. Vignali^{3,5}, and L. Zappacosta²

¹ IRAM - Institut de RadioAstronomie Millimétrique, 300 rue de la Piscine, 38406 Saint Martin d'Hères, France, e-mail: feruglio@iram.fr

² INAF - Osservatorio astronomico di Roma, via Frascati 33, 00040 Monteporzio Catone, Italy

³ University of Bologna, Department of Physics and Astronomy, viale Berti Pichat 6/2, 40127 Bologna, Italy

⁴ Max Planck Institut für Extraterrestrische Physik, Giessenbachstrasse 1, 85748 Garching bei München, Germany

⁵ INAF - Osservatorio Astronomico di Bologna, via Ranzani 1, 40127 Bologna, Italy

⁶ Laboratoire AIM, CEA/DSM-CNRS-Université Paris Diderot, Irfu/Service d'Astrophysique, CEA Saclay, Orme des Merisiers France, 91191 Gif-sur-Yvette Cedex, France

⁷ Departamento de Ciencias Físicas, Universidad Andres Bello, Av. Republica 252, Santiago, Chile

⁸ KAVLI

⁹ Astronomy Centre, Dept. of Physics and Astronomy, University of Sussex, Falmer, Brighton BN1 9QH, UK

February 23, 2014

ABSTRACT

Context. Understanding the relationship between the formation and evolution of galaxies and their central super massive black holes (SMBH) is one of the main topics in extragalactic astrophysics. Links and feedback may reciprocally affect both black hole and galaxy growth.

Aims. Observations of the CO line at redshifts of 2-4 are crucial to investigate the gas mass, star formation activity and accretion onto SMBHs, as well as the effect of AGN feedback. Potential correlations between AGN and host galaxy properties can be highlighted by observing extreme objects. Despite their luminosity, hyper-luminous QSOs at $z = 2 - 4$ are still little studied at mm wavelengths.

Methods. We targeted CO(3-2) in ULAS J1539+0557, an hyper-luminous QSO ($L_{\text{bol}} > 10^{48}$ erg/s) at $z = 2.658$, selected through its unusual red colors in the UKIDSS Large Area Survey (ULAS).

Results. We find a molecular gas mass of $4.1 \pm 0.8 \times 10^{10} M_{\odot}$, and a gas fraction of $\sim 0.4-0.1$, depending mostly on the assumed source inclination. We also find a robust lower limit to the star-formation rate ($\text{SFR} = 250-1600 M_{\odot}/\text{yr}$) and star-formation efficiency ($\text{SFE} = 25-350 L_{\odot}/(\text{K km s}^{-1} \text{pc}^2)$) by comparing the observed optical-near-infrared spectral energy distribution with AGN and galaxy templates. The black hole gas consumption timescale, $M(\text{H}_2)/\dot{M}_{\text{acc}}$, is ~ 160 Myr, similar or higher than the gas consumption timescale.

Conclusions. The gas content and the star formation efficiency are similar to those of other high-luminosity, highly obscured QSOs, and at the lower end of the star-formation efficiency of unobscured QSOs, in line with predictions from AGN-galaxy co-evolutionary scenarios. Further measurements of the (sub)-mm continuum in this and similar sources are mandatory to obtain a robust observational picture of the AGN evolutionary sequence.

Key words. Galaxies: active – Galaxies: evolution – Galaxies: quasars – general

1. Introduction

Understanding the relations between the formation and evolution of galaxies and their central super massive black holes (SMBH) is a major challenge of present-day astronomy. Most of galaxy assembly and accretion activity occur at $z = 2 - 4$, so it is crucial to study SMBH-galaxy relationships at this epoch. The two main open questions are: a) what is the mechanism triggering nuclear accretion and star-formation? and b) are AGN outflows truly able to regulate star-formation in their host galaxies? Observations of molecular gas are useful to address both questions. So far, molecular gas has been detected in a few tens of $z > 2$ QSOs, with typical masses $1 - 10 \times 10^{10} M_{\odot}$, indicating gas-rich hosts. However, most of these observations have been done either on lensed object (where the intrinsic luminosity is magnified up to 1000 times), or on $z = 5 - 6$ QSOs (Riechers 2011 and references therein).

There is a growing evidence for two modes of star-formation which may also be relevant for triggering nuclear activity: a quiescent one, taking place in most star-forming galaxies, with gas conversion time scales of ~ 1 Gyr, and a less common *star-burst* mode, acting on much shorter time scales ($\sim 10^7 - 10^8$ yr, see e.g. Rodighiero et al. 2011, Lamastra et al. 2013a and references therein). The latter mode is likely related to the powering of high luminosity QSOs. In fact, bolometric luminosities of the order of $10^{47} - 10^{48}$ ergs/s imply mass accretion rates of tens to hundreds M_{\odot}/yr onto $10^9 - 10^{10} M_{\odot}$ SMBHs (assuming a radiative efficiency of 0.1). If the accretion lasts for a few tens Myr (Salpeter timescale), this in turn implies gas reservoirs of $10^9 - 10^{10} M_{\odot}$ even if the fraction of the gas that can reach the nucleus is high ($\Delta M_{\text{gas}} \sim M_{\text{gas}}/5$). At present, galaxy interactions seem to be the best (if not the only) mechanism capable of destabilizing such huge gas masses on short time scales. This naturally produces powerful AGN hosted in star-burst galaxies (Lamastra et al 2013b). In principle, from the gas consumption timescale (or its inverse, the so-called star formation efficiency, SFE, i.e. the ratio between the star-formation rate and the gas mass), one can

* Based on observations carried out with the IRAM Plateau de Bure Interferometer. IRAM is supported by INSU/CNRS (France), MPG (Germany) and IGN (Spain).

directly derive information on the AGN and star-formation triggering mechanisms.

The SFE depends also on the SMBH gas consumption time scales and on the energy injected in the ISM by the AGN (*feedback*). High SFE may be the outcome of a small cold gas reservoir which was reduced by on-going SMBH accretion and consequent AGN feedback. For this reason, to have information on AGN feedback is crucial for addressing both questions. There is both theoretical and observational evidence that high luminosity QSOs drive powerful outflows. On the theoretical ground, physically-motivated models predict strong winds from AGN with SMBH larger than $10^8 M_{\odot}$ (Zubovas & King 2014 and references therein). These models in general predict mass flows proportional to the AGN bolometric luminosity to some power (e.g. $M_{out} \propto L_{bol}^{1/2}$ in the Menci et al. 2008 model). For these reasons, the most luminous QSOs in the Universe are ideal and unique targets to study AGN/galaxy feedback mechanisms regulated by powerful outflows. Powerful and massive AGN driven outflows of molecular gas were recently discovered in luminous QSOs (Maiolino et al. 2012, Feruglio et al. 2010, Ciccone et al. 2013). Broad Absorption Lines (BAL) with outflow velocities up to several thousands km/s are common in high-luminosity QSOs (Borguet et al. 2013). BALs are found in 40% of mid-infrared selected QSOs (Dai et al. 2008) and in 40% of the *WISE* selected luminous QSOs (Bongiorno et al. 2014, in prep.). Powerful, galaxy wide outflows have also been found in ionized gas using the broad [OIII] emission line (Cano-Diaz et al. 2012).

In this paper we present results from the first Plateau de Bure Interferometer (PdBI) observation of an hyper-luminous QSO, selected from the UKIDSS Large Area Survey (ULAS) and the VISTA (J, K bands) Hemisphere Survey: ULAS J1539+0557 at $z = 2.658$ (ra:15:39:10.2, dec: 05:57:50.0, Banerji et al. 2012). ULAS J1539+0557 is heavily reddened (rest frame $A_V \sim 4$) and has a bright $22 \mu\text{m}$ flux of 19 mJy in the *WISE* all-sky survey, corresponding to $\lambda L_{\lambda}(7.8 \mu\text{m}) = 10^{47}$ ergs/s, and a bolometric luminosity of $L_{bol} \sim 10^{48}$ erg/s. The black hole mass is as large as $7.4 \times 10^9 M_{\odot}$. As detailed in Banerji et al. (2012a), these hyper-luminous QSOs are unlikely to be lensed, therefore they truly trace an extremely luminous population.

In the following we present the results of 3 mm observations of ULAS J1539+0557, targeting the CO(3-2) transition. We derive the gas mass, dynamical mass, and star-formation rate (SFR) of the host galaxy through the comparison of the observed UV-MIR Spectral Energy Distribution (SED) with galaxy templates. We compare the observed gas masses, gas fraction and gas consumption timescale with those of the other QSOs and galaxies at similar redshift. We finally discuss future desirable developments in this topic. A $H_0 = 70 \text{ km s}^{-1} \text{ Mpc}^{-1}$, $\Omega_M = 0.3$, $\Omega_{\Lambda} = 0.7$ cosmology is adopted throughout.

2. Millimeter observations and results

ULAS J1539+0557 was observed at a frequency of 94.5 GHz with the PdBI array in the most compact (D) configuration, in September 2013. The system temperature was between 80 and 120 K, and water vapor about 5 mm. The quasar 1546+027 (1.8 Jy at 94.5 GHz) was used as a phase and amplitude calibrator. The quasar 3C454.3 (10.1 Jy) was used for bandpass and absolute flux calibration. We estimate a 10% error on the absolute flux calibration. Calibration and mapping were done in the GILDAS environment. The flagging of the phase visibilities was fixed at 35% rms in order to maximize the signal to noise ratio (S/N) of the detection. This flagging yields a 1σ sensitivity of

0.3 mJy/beam in 79 MHz channels, and a total 6 antenna equivalent on-source time of 3.2 hours. With natural weighting, the synthesized beam is 8.9 by 5.0 arcsec.

Fig. 1 shows the spectrum and collapsed map of ULAS J1537+0557. The CO(3-2) emission line is detected at a confidence level of 5.4σ (0.5, 0.3 arcsec offset from the phase center, based on the fit of the visibilities in the uv plane adopting an unresolved source model) and lies at the frequency expected based on the optical spectroscopic redshift. The integrated flux of the line is 1.37 Jy km/s over the full line width (from fitting of the visibilities by a Gaussian function). L'_{CO} can be estimated by extrapolating to the CO(1-0) luminosity from the CO(3-2) flux, using excitation models of high- z QSOs (Riechers et al. 2006, Riechers 2011). The observed scatter (see e.g. Carilli & Walter 2013) is of the same order of magnitude as the relative error on the CO flux of ULAS J1539+0557, and therefore we neglect it in the following estimates. We then find a line luminosity $L'_{CO} = (5.1 \pm 1.2) \times 10^{10} \text{ K km/s pc}^2$. By using a conversion factor $X_{CO} = 0.8$ (e.g. Carilli & Walter 2013), we derive a total molecular gas mass of $M(H_2) = (4.1 \pm 0.8) \times 10^{10} M_{\odot}$. The 3 mm continuum is not detected (with a 3σ upper limit of 0.1 mJy).

The CO(3-2) line profile in Fig. 1 is broad. Fitting the profile over the full velocity range with a single Gaussian component we obtain a FWHM is $1600 \pm 700 \text{ km/s}$. This would be the highest FWHM among high- z QSOs (average is $\sim 300 \text{ km/s}$, Riechers 2011). Although noisy, the line profile in Fig. 1 appears asymmetric, skewed toward positive velocities. The feature at positive velocities might either be a different component of the emission or noise. If we exclude from the fit velocities $> 500 \text{ km/s}$ the best fit line width is narrower, $\text{FWHM} = 840_{-350}^{+1000} \text{ km/s}$. Fitting the profile with two Gaussian functions we obtain a best fit solution with a main component centered at zero velocity with $\text{FWHM} = 1100 \pm 450 \text{ km/s}$ and a second, fainter component centered at about 1200 km/s. This would suggest that the complex line profile is the result of a merging system (see e.g. Fu et al. 2013). The S/N of the data is not good enough to disentangle between the different possibilities. In the following we conservatively assume that the FWHM of the line is $840_{-350}^{+1000} \text{ km/s}$.

The source appears unresolved, but the limits on its extension are quite loose (physical size $< 40 \text{ kpc}$) because of the large synthesized beam.

The CO line width can be converted into a dynamical mass assuming a size R and an inclination i of a rotating molecular gas disc. We derive the product of the circular velocity at the outer CO radius v_c times the sinus of inclination, $v \times \sin(i)$, by dividing the FWHM of the CO line by 2.4 (Tacconi et al. 2006). The dynamical mass can then be estimated as $M_{dyn} \sin^2(i) = R \Delta v_c^2 / G = 5.7 \times 10^{10} M_{\odot}$, assuming $R = 2 \text{ kpc}$, a value commonly used for QSOs (e.g. Coppin et al. 2008), similar to that measured for the molecular disc of the $z=4.694$ southern AGN of BR1202-0725 (Carniani et al. 2013), or the lower luminosity QSOs (Krips et al. 2007), or local QSOs (e.g. Mark231, Downes & Solomon 1998), and similar to that found in SMGs (Tacconi et al. 2006, 2008).

Table 1 compares CO line FWHM, gas and dynamical mass of ULAS J1539+0557 to those of the only other three available $z > 2$, hyper-luminous ($\lambda L_{\lambda}(7.8 \mu\text{m}) \geq 10^{47}$ ergs/s) QSOs.

The large FWHM of CO(3-2) of ULAS J1539+0557 suggests a non negligible inclination. If $i = 20 \text{ deg}$, as in SBSJ1408+567 (Coppin et al. 2008), $M_{dyn} \sim 5 \times 10^{11} M_{\odot}$, if $i=45 \text{ deg}$, $M_{dyn} \sim 10^{11} M_{\odot}$. The ratio between the gas mass and the dynamical mass M_{H_2}/M_{dyn} is therefore likely in the range 0.4-0.1.

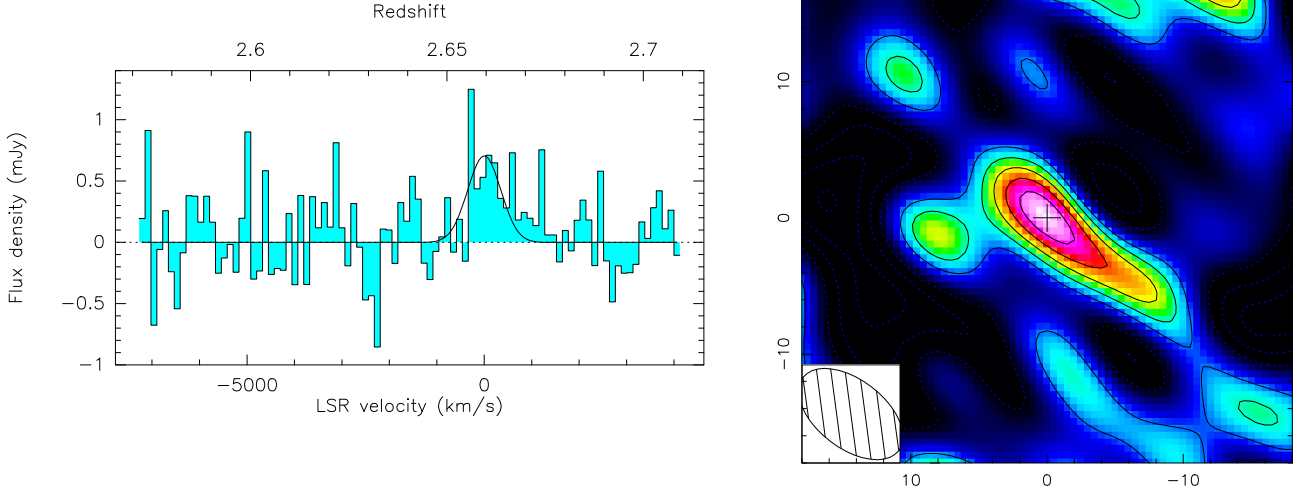


Fig. 1. Left panel: spectrum of ULAS J1539+0557 integrated over the beam. The solid line shows the Gaussian fit with $\text{FWHM}=840^{+1000}_{-350}$ km/s, and centered at the frequency corresponding to the redshift of the source. Right panel: integrated map of CO(3-2). Contour levels are 1σ each ($\sigma = 0.2$ mJy). The synthesized beam is shown in the bottom-left corner.

3. Spectral Energy Distribution

ULAS J1539+0557 has never been observed at far infrared or sub-mm wavelengths. It is possible, however, to compile a robust broad-band spectral energy distribution (SED) from the UV to the $22\ \mu\text{m}$ band (photometry from Banerji et al. 2012). The source is undetected in the FIRST VLA survey (Becker et al. 2012), the 3σ upper limit is 0.375 mJy at 20 cm. The SED in the QSO rest frame is shown in Fig. 2. The SED at rest-frame wavelengths above $\sim 4000\ \text{\AA}$ is clearly dominated by the AGN. The emission of the AGN rapidly drops below $3000\ \text{\AA}$, indicating that the nuclear emission is substantially obscured, consistent with the color selection of this source in the VISTA survey (Banerji et al. 2012). The SED below $3000\ \text{\AA}$ is likely dominated by starlight from the host galaxy. Translating the observed $1500\ \text{\AA}$ luminosity into a SFR, assuming the Madau (1998) conversion and zero galaxy extinction, provides a firm lower limit to the host galaxy SFR of $70\ M_{\odot}/\text{yr}$. The real SFR is probably much higher than this value, if the galaxy is substantially obscured by dust, but difficult to constrain due to the lack of far-IR data.

To obtain a better SFR estimate, we modeled the broad band, $0.1\text{--}6\ \mu\text{m}$ SED by using a library of AGN and galaxy templates (Bongiorno et al. 2012). For the AGN component, we used the mean QSO SED from Richards et al. (2006), while for the galaxy component, a library of synthetic spectra generated using the stellar population synthesis models of Bruzual & Charlot (2003) has been adopted. Both the AGN and the galaxy templates can be affected by dust extinction. For a given galaxy template, the free parameters in the fit are thus normalization and extinction of both AGN and galaxy templates. We accepted solutions with galaxy stellar masses smaller than $10^{12}\ M_{\odot}$ and $\text{SFR} \times \text{duration}$ of the starburst \lesssim total stellar mass. The best fit values are $400\ M_{\odot}/\text{yr}$ of SFR and $3 \times 10^{10}\ M_{\odot}$ for the stellar mass. The 1σ confidence intervals for SFR and stellar mass are $250\text{--}1600\ M_{\odot}/\text{yr}$ and $3 \times 10^{10}\text{--}3 \times 10^{11}\ M_{\odot}$ respectively. The best fit extinction for the AGN and the galaxy is $E(B-V) = 1.1$ and 0.2 , respectively.

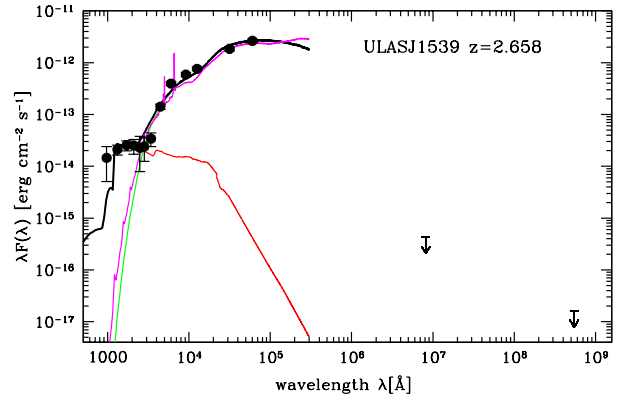


Fig. 2. The optical to radio wavelength rest-frame SED of ULAS J1539+0557 fitted with 2 components: a highly extinguished AGN model ($E(B-V)=1.1$, magenta line), and a galaxy component (with different extinction, $E(B-V)=0.2$, red line). The black solid line shows the sum of the two components. The arrows indicate the 3σ upper limits in the continuum at 3 mm (these observations) and at 20 cm from the FIRST survey.

4. Discussion

ULAS J1539+0557 is an extreme object, with a bolometric luminosity of $L_{\text{bol}} = 1.6 \times 10^{48}$ erg/s (derived from the $5100\ \text{\AA}$ continuum), and a SMBH mass, estimated from $H\alpha$ emission line, as large as $7.4 \times 10^9\ M_{\odot}$ (Banerji et al. 2012). This implies that the SMBH is accreting at the Eddington limit, at a rate of $dm/dt = 200\text{--}300\ M_{\odot}/\text{yr}$. At this rate, the black hole gas consumption timescale, $M(\text{H}_2)/M_{\text{acc}}$, would be only ~ 160 Myr.

In the following we discuss the source properties in comparison with other known luminous systems. A clean estimator for the intrinsic AGN power is its mid-infrared luminosity, since it guarantees little bias against dusty objects and little extinction (or absorption) corrections. Recently, the *WISE* satellite has performed the deepest all-sky survey at $22\ \mu\text{m}$, which samples the

Table 1. Hyper-luminous QSOs at $z > 2$

QSO	z	$\lambda L_{\lambda}(7.8 \mu\text{m})$ [10^{47} ergs/s]	$M(\text{H}_2)$ [$10^{10} M_{\odot}$]	FWHM [km/s]	$M_{\text{dyn}} \sin^2(i)$ [$10^{10} M_{\odot}$]	$M_{\text{H}_2}/M_{\text{dyn}}$	M_{BH} [$10^9 M_{\odot}$]	Ref
ULAS J1539+0557	2.658	1.0	4.1 ± 0.8	840^{+1000}_{-350} (3-2)	5.7^a	$0.4-0.1^d$	7.4	(1)
RXJ1249-0559	2.247	1.7	2.9 ± 0.8	1090 ± 340 (3-2)	9.7^a	0.30^b	5.7	(2)
SBSJ1408+567	2.583	1.8	6.0 ± 0.5	311 ± 28 (3-2)	0.78^a	0.90^c	1.1	(3)
BR1202-0725	4.694	1.6	3.2 ± 1.2	363 ± 37 (5-4)	0.83	0.25^e	1.5	(4,5)

^aassuming a disk radius of 2 kpc; (1) Banerji et al. 2012; (2) Coppin et al. 2008, (3) Beelen et al. 2004; (4) Salome et al. 2012; (5) Carniani et al. 2013, ^b likely high inclination; ^c assuming $i = 20$ deg; ^d assuming $i = 45$ deg and $i = 20$ deg; ^e assuming $i = 15$ deg.

rest frame 4-8 μm band at $z = 2 - 4$ (where AGN heated warm dust is the main component to the total flux), finding the most luminous AGN in the sky at $z < 4 - 5$. It is therefore convenient to use the 7.8 μm luminosity ($\lambda L_{\lambda}(7.8 \mu\text{m})$) as a reliable proxy for the AGN power. By measuring $\lambda L_{\lambda}(7.8 \mu\text{m})$ of all QSOs with CO detections, we find that only three of these sources at $z < 5$ have extreme intrinsic luminosities ($\lambda L_{\lambda}(7.8 \mu\text{m}) \geq 10^{47}$ ergs/s). Other six QSOs with CO detection have $10^{46} < \lambda L_{\lambda}(7.8 \mu\text{m}) < 10^{46.5}$ ergs/s, including the two highly obscured SWIRE QSOs of Polletta et al. (2011). To characterize quantitatively the unique population of hyper-luminous QSOs we need to substantially increase the sample with gas mass, dynamical mass and SFR detections.

Fig. 3 plots L'_{CO} against $\lambda L_{\lambda}(7.8 \mu\text{m})$ for a compilation of both unobscured and highly obscured AGN. The luminosities of lensed object have been corrected for the published lens amplification factor. A rough correlation between the AGN luminosity and the CO luminosity is present. Note that the scatter in the correlation is higher for the lensed objects, likely due to the fact that both luminosities have been corrected for the same amplification factor, but the source of the 7.8 μm luminosity is most likely very compact (pc scale), while the source of the CO luminosity could be more extended (a few kpc), implying an amplification pattern more complex than the assumed one. The 7.8 μm luminosities of highly obscured (Compton Thick, $N_{\text{H}} > 10^{24} \text{ cm}^{-2}$, two are from Polletta et al. 2011, and Mrk231) have been computed using the 6.5-22 μm fluxes, not corrected for extinction, which however may be relevant in highly obscured objects even at such long wavelengths. AGN at $z > 5.8$ are found at the lower part of the correlation. Non-lensed QSOs at $z = 1.5 - 5$ with $\lambda L_{\lambda}(7.8 \mu\text{m}) > a$ few 10^{46} ergs/s have all high L'_{CO} , in the range $3 - 8 \times 10^{10} \text{ K km/s pc}^2$.

To convert L'_{CO} into gas mass we again adopt a conversion factor $X_{\text{CO}} = 0.8$, as in most studies of AGN, ULIRGs and SMGs (see Carilli & Walter 2013). The molecular gas mass of ULAS J1539+0557 and three other hyper-luminous QSOs (Table 1) are in the range $3-6 \times 10^{10} M_{\odot}$. We evaluate the dynamical mass of ULAS J1539+0557 under admittedly major assumptions (the FWHM estimated from the core of the CO(3-2) line, the size of the molecular gas disc of 2 kpc and its inclination angle). We find that the gas mass is 0.1-0.4 of the dynamical mass. This suggests that the host galaxy of this hyper-luminous QSO is not deprived from gas, and it is likely forming stars actively, in agreement with the prediction of semi-analytic models for AGN/galaxy co-evolution (Lamastra et al. 2013b).

SFE is usually computed as $\text{SFE} = L_{\text{FIR}}/L'_{\text{CO}}$. Since ULAS J1539+0557 has never been observed at far infrared (FIR) or sub-mm wavelengths, we do not have a direct measure of L_{FIR} . We can, however, estimate L_{FIR} from the SFR obtained from the SED fitting, using the conversion $\text{SFR} = 2 - 1.2 \times 10^{-10} (L_{\text{FIR}}/L_{\odot}) M_{\odot}/\text{yr}$ (Scoville 2012). We find SFE between 25 and 350 $L_{\odot}/(\text{K km s}^{-1} \text{ pc}^2)$, which correspond to a gas consumption timescale of

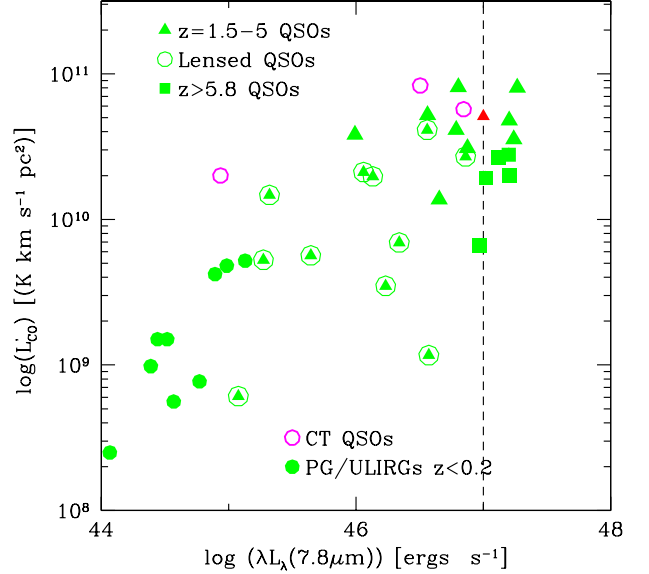


Fig. 3. L'_{CO} versus $\lambda L_{\lambda}(7.8 \mu\text{m})$ for a compilation of AGN. The red triangle corresponds to ULAS J1539+0557.

25-160 Myr, smaller or equal to the black hole gas consumption timescale computed above (assuming that AGN feedback has not yet been able to significantly modify its environment and reduce the total host galaxy cold gas mass).

For a SFR in the range 250-1600, the ratio $\dot{M}_{\text{acc}}/\text{SFR}$ is in the range 0.1 - 1, which is $\sim 2 - 3$ orders of magnitude above the mean value 10^{-3} found by Mullaney et al. (2012) for AGN with star-forming hosts in GOODS-S, thus suggesting that ULAS J1539+0557 is an outlier to the "AGN main sequence". The SMBH mass is $\geq 2\%$ of the dynamical mass, so M_{BH}/M_* is of the order 0.1 or higher, i.e. 2 orders of magnitude larger than the canonical value. This means that, although ULAS J1539+0557 has a extremely massive SMBH, this seems to live in an ordinary galaxy host with $M_{\text{dyn}} \sim 10^{11} M_{\odot}$, which is uncommon at this redshift, but not as such at higher redshift. Stochastic fluctuations between SMBH and SF activity, as advocated by Mullaney et al. (2012), are unlikely to give rise to such extreme outliers.

In Fig. 4 we plot the SFE against redshift (left panel) and L_{FIR} against L'_{CO} (right panel), for a compilation of AGN and galaxies (samples of Daddi et al. 2007, Genzel et al. 2000, Riechers et al. 2011 and references therein, Krips et al. 2012). The uncertainty on L_{FIR} and SFE, due to both the uncertainty on the evaluation of the SFR from SED fitting, and that associated to the conversion from SFR to L_{FIR} , prevents us from precisely locating ULAS J1539+0557 in the $L_{\text{FIR}}-L'_{\text{CO}}$ plane. Its FIR luminosity is consistent with both the locus of normal, star-forming galaxies and that of SMGs, ULIRGs and luminous

QSOs. At face value, the SFE of ULAS J1539+0557 is lower than (although still statistically consistent) that of other luminous QSOs at similar or lower redshift (Riechers et al. 2011). It is similar to that of other highly obscured, but less extreme AGN. For example, Krips et al. (2012) found $SFE \sim 100 - 200$ in nearby type 2 QSOs, and Polletta et al. (2011) found similar SFE in two galaxies hosting high-luminosity, obscured QSOs at $z \sim 3$. Therefore ULAS J1539+0557 may be an extreme case of a dust enshrouded, hyper-luminous QSO.

In the AGN/galaxy coevolution scenario obscured AGN may be an early phase of the life cycle of luminous quasars (Sanders et al. 1988, Menci et al. 2008 and references therein), in which the strong AGN outflows have not yet cleared the host galaxy from most of its gas and dust, thus resulting in a lower SFE than that of unobscured quasars. Conversely, luminous unobscured QSOs may be caught at the end of this process, and have high SFE because the AGN feedback has been already efficient in expelling a large fraction of the gas. The uncertainties on the SFR and SFE of ULAS J1539+0557 are, however, too large to allow a firm conclusion.

5. Conclusions

We detected CO(3-2) in the hyper-luminous QSO ULAS J1539+0557 at $z = 2.658$, a source selected by extremely red colors in the UKIDSS Large Area Survey (ULAS) and bright at 22 micron in the *WISE* survey. We find a molecular gas reservoir of $4.1 \pm 0.8 \cdot 10^{10} M_{\odot}$. The dynamical mass is not well constrained but it could be 2-10 times higher, depending mostly on the gas disk size and inclination. In any case, the host galaxy does not appear deprived from cold gas, suggesting that it is still forming stars actively. From fitting of the UV to mid-IR SED, we derived a robust lower limit to the SFR and gas consumption time scale. The ratio of SMBH accretion to star-formation rate, \dot{M}_{acc}/SFR , is significantly higher than that found by Mullaney et al. (2012) for AGN with star-forming hosts. The SFE is similar to that of highly obscured, high luminosity QSOs. This class of QSOs is believed to witness the brief evolutionary phase that traces the transition from a heavily enshrouded ULIRG-like phase of black-hole growth to the blue unobscured quasars. Due to their high luminosity these exceptional objects are ideal laboratories to investigate the physics of the feedback phenomenon with in situ observations at the peak of galaxy and SMBH assembly. The high luminosity allows highlighting the correlation between SFE and other parameters (e.g. obscuration, AGN luminosity).

Both the *WISE* all sky survey and the UKIDSS and VISTA hemisphere Surveys have revealed a population of hyper-luminous QSOs in near and mid infrared. These selections have already produced reasonably large hyper-luminous QSO samples at $z \sim 1.5 - 4$, the main epoch of galaxy formation and accretion activity in the Universe. Recently, Banerji et al. (2014) presented IR and X-ray observations of a similar source from the same parent sample, ULAS J1234+0907 at redshift 2.5, finding high SFR ($\approx 2000 M_{\odot}/yr$) and high X-ray luminosity ($\approx 10^{45} \text{ ergs/s}$), thus confirming that infrared selection is efficient in discovering a population of hyper-luminous QSOs in the *blowout* phase.

It is urgent to increase the sample of hyper-luminous QSOs with good estimates of both gas mass, dynamical mass, L_{FIR} , and X-ray luminosity, including both unobscured and highly obscured QSOs. These goals can be achieved with the present and future generation of millimeter interferometers, such as the PdBI, NOEMA and ALMA.

Acknowledgements. FF, AB and CF acknowledge support from PRIN-INAF 2011. MB acknowledges support from the FP7 Career Integration Grant "eEASy" (CIG 321913). IG acknowledges support from FONDECYT through grant 11110501.

References

- Banerji, M., McMahon, R. G., Hewett, P. C., Gonzalez-Solares, E. and Kaposov, S. E. MNRAS, 429L, 55
- Banerji, M., Fabian, A. C. and McMahon, R. G. 2014 MNRAS, tmpL, 9
- Becker, R. H., Helfand, D. J., White, R. L., Gregg, M. D. and Laurent-Muehlheisen, S. A. 2012, yCat, 8090, 0B
- Bongiorno, A., Merloni, A., Brusa, M. Magnelli, B., Salvato, M. et al. 2012, MNRAS, 527, 3103
- Borguet, B. C. J., et al., 2013, ApJ, 762, 49
- Carilli, C. L. and Walter, F. 2013, ARA&A 51, 105
- Carniani, S., Marconi, A., Biggs, A., Cresci, G., Cupani, G. et al. 2013 A&A 559A, 29
- Cicone, C., Feruglio, C., Maiolino, R., Fiore, F., Piconcelli, E., Menci, N. et al. 2012, A&A in press, arXiv1204.5881C
- Daddi, E., Elbaz, D., Walter, F., Bournaud, F., Salmi, F. et al. 2010, ApJ, 714, 118
- Dai, X., Shankar, F. and Sivakoff, G. R. 2008, ApJ 672, 108
- Downes, D. and Solomon, P. M. 1998, ApJ 507, 615
- Faucher-Figuere, C-A. & Quataert, E. 2012, MNRAS, 425, 605
- Feruglio, C., Maiolino, R., Piconcelli, E., Menci, N., Aussel, H. et al. 2010, A&A 518, 155
- Genzel, R., Baker, A. J., Tacconi, L., Lutz, D., Cox, P. et al. 2003, ApJ, 584, 633
- Genzel, R., Tacconi, L., Gracia-Carpio, J., Sternberg, A., Cooper, M.C. et al. 2010, MNRAS, 407, 209
- King, A. R. 2010, MNRAS, 402, 1516
- Krips, M., Neri, R., Garcia-Burillo, S., Martin, S., Combes, F. et al. 2008, ApJ, 677, 262
- Krips, M., Neri, R. and Cox, P. 2012, ApJ 753, 135
- Lamastra, A., Menci, N., Fiore, F. and Santini, P. 2013, A&A 552A, 44
- Lamastra, A., Menci, N., Fiore, F., Santini, P. Bongiorno, A. et al. 2013, A&A, 559A, 56
- Madau, P. et al 1998,
- Maiolino, R., Gallerani, S., Neri, R., Cicone, C., Ferrara, A. et al. 2012, MNRAS 425, 66
- Menci, N., Fiore, F., Puccetti, S. & Cavaliere, A. 2008, ApJ, 686, 219
- Polletta, M., Nesvadba, N. P. H., Neri, R., Omont, A., Berta, S et al., 2011 A&A, 533A, 20
- Richards, G. T., Lacy, M. Storrie-Lombardi, L. J. et al. 2006, ApJS 166, 470
- Riechers, D. A., Walter, F., Carilli, C. L., Knudsen, K. K., Lo, K. Y., et al. 2006, ApJ 650, 604
- Riechers, D. A. 2011, ApJ 730, 108
- Riechers, D. A., Carilli, C. L., Maddalena, R. J., Hodge, J., Harris, A. I., Baker, A. J. et al. 2011, ApJ, 739, 32
- Rodighiero, G., Daddi, E., Baronchelli, I. Cimatti, A., Renzini, A. et al. 2011, ApJ, 739L, 40
- Sanders, D. B., Soifer, B. T., Elias, J. H., Madore, B. F., Matthews, K. et al., 1988, ApJ, 325, 74
- Solomon, P. M. et al. 1997, ApJ 478, 144
- Tacconi, L., Neri, R., Chapman, S. C., Genzel, R. Smail, I. et al. 2006 ApJ, 640, 228
- Tacconi, L., Genzel, R., Smail, I., Neri, R., Chapman, S.C., et al. 2008, ApJ 680, 246
- Zhang, K., Dong, X., Wang, T. and Gaskell, C. M. 2011, ApJ, 737, 71
- Zubovas, K. & King A. 2012, ApJ, 745, 34
- Zubovas, K. & King A. 2014, MNRAS in press, arXiv:1401.0392

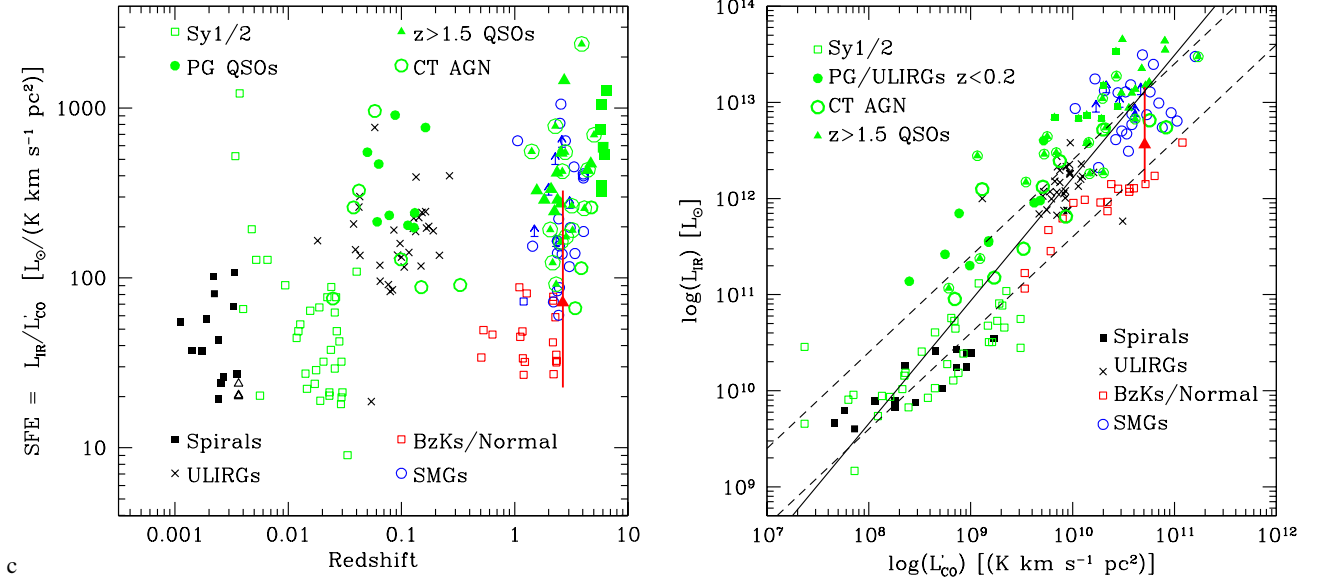


Fig. 4. [Left panel]: SFE versus redshift for a compilation of AGN and star-forming galaxies (from Daddi et al. 2007, Genzel et al. 2010, Riechers et al. 2011 and references therein, Krips et al. 2012). The red triangle corresponds to ULAS J1539+0557. [Right panel]: L_{FIR} versus L_{CO} for a compilation of AGN and star-forming galaxies at all redshifts. The red triangle corresponds to ULAS J1539+0557. The solid line is a fit to all data, the dashed lines are the best fit for main sequence galaxies and star-burst galaxies (Daddi et al. 2010, Genzel et al. 2010).